

## EXPERIMENTAL INVESTIGATION ON THE FLOW INDUCED BY ARTIFICIAL CILIA IN MICRON-SIZED CHANNELS

**Jeanette Hussong\***, Jerry Westerweel,  
Leeghwaterstraat 21, 2626CA, Delft, The Netherlands,  
j.hussong@tudelft.nl, j.westerweel@tudelft.nl

**Jacob Belardi, Nicolas Schorr,**  
Georges Koehler Allee 103, 79110 Freiburg, Germany,  
belardi@imtek.de, schorr@imtek.de

**Bogdan Craus**  
Philips Research Laboratories, High Tech Campus 12<sup>a</sup>, 5656AE Eindhoven, The Netherlands, bogdan.craus@philips.com

### Key words

Cilia, μPIV, biomimetic pumping

### Abstract

*A new biomimetic pumping method of beating artificial cilia is investigated. The artificial cilia were actuated externally with an external magnetic field in a micro channel. Micro-PIV measurements were performed to quantify the cilia-induced fluid transport. Cilia actuated with a spatially homogeneous magnetic field induced an oscillatory fluid motion in the micro-channel, but no significant fluid transport. We believe that this is due to the fact that the cilia are stiff and only perform a rotational motion around their fixation point. On the other hand, cilia actuated in an inhomogeneous magnetic field induced a time-averaged net flow of approximately 100 μm/s in a plane 60 μm above the channel wall was measured at 20Hz actuation. It is anticipated that a net fluid transport takes place due to a combination of an asymmetric beat cycle and a temporary-induced phase lack between beating cilia. Phase locked measurements showed that the flow is strongly oscillatory during each actuation cycle exhibiting a temporary flow reversal at a cilia close measurement plane. A cilia-induced volume flow rate was calculated from the velocity profile that was measured over the channel height. If no back-pressure is build up the cilia-induced volume flow rate is in the order of 10-20 μl/min.*

### 1. Introduction

The rapid development of miniaturization in chemical synthesis, bio-medical research and other applications generates a growing need for alternative methods of manipulating fluids on sub-millimeter scales. In technical applications fluids in micron-sized channels are normally driven by volume or mass flow controlled external mechanical pumps. However, nature teaches us that there exist other, very efficient ways to mechanically pump fluids in micron-sized channels

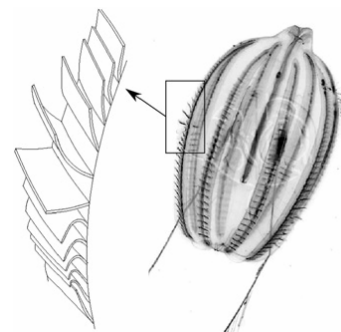


Fig.1: Propulsive row of cilia on a pleurobrachia (Dauplain et al., 2008)

such as by a peristaltic motion of the channel walls or by the beating of micron sized, wall-attached hair-like cell extensions, so-called cilia. Cilia occur in organs such as the trachea to transport liquids and they are often used by aquatic microorganisms for propulsion (see Fig. 1).

Cilia have been studied for almost 200 years. Investigations done by Purkinje and Valentin in the 19th century have been thoroughly reviewed by Teich et al. (1970). Due to length scales, natural cilia can be interpreted as a Stokes flow pump. They perform a paddling motion which consists of an effective stroke where the cilium is stretched and a recovery stroke during which the cilium bends to reduce its drag while moving back to its initial position. This induces a net fluid transport in viscous flows (Purcell, 1977).

In nature, adjacent cilia beat slightly out of phase. The phase shift of the beat circle of neighboring cilia results in traveling waves that move over the cilia tip surface, called metachronal wave. Experimental studies on cilia propulsion in the airways has been performed by Knowles and Boucher (2002); Matsui et al. (1998); Kummer et al. (2009) and others. The flow induced by a frog's upper digestive tract has been shown to generate flow in water up to several hundreds of micrometers above its surface (Wilson et al., 1975) and recently, rapid cilia-driven bead transport has been measured over dissected and mucus freed trachea sections of mice (Koenig et al., 2009; Klein et al., 2009).

A huge number of numerical investigations were performed on cilia propulsion and pumping and can be divided according to three main groups of models: the discrete cilia models, the cilia envelope models and the cilia sublayer models. Most discrete cilia models served to exploring the interaction and metachronal coordination of cilia in the Stokes regime (Gueron et al., 1997; Gueron et al., 1998; Lenz and Ryskin, 2006; Vilfan et al., 2006; Niedermayer et al., 2008). In discrete models that focus on the flow field, cilia forces are implemented into the momentum equations making use of the Immersed Boundary Methods (Dillon et al., 2006; Dillon et al., 2007; Dauplain et al., 2008; Heys et al., 2008). The envelope models are based on the infinite waving sheet theory developed by Taylor (1951) and they are usually used to simulate multi-cilia systems (Blake et al., 1971; Tuck et al., 1968; Nielsen and Larsen, 1993; Brennen, 1974; Katz, 1974). Sublayer models represent a cilia covered surface as fully submerged interlayer of beating structures. The first discrete sublayer model by Blake (1972) was soon extended (Liron and Mochon, 1976; Liron, 1978) and used to simulate mucociliary transport (Smith et al., 2007). The continuum sublayer model is also called traction layer model and was used in early stages by Barton and Raynor (1967), Keller and Wu (1977) and Blake and Winet (1980). Non-Newtonian effects of the mucus layer were considered in later traction layer models by King et al. (1993) and Smith et al. (2007).

By nature inspired an increased effort is nowadays undertaken to investigate artificial cilia-induced fluid manipulation and transport. Numerical studies have been performed by Wilderbeek and Khaderi which show that artificial cilia actuated by an external electromagnetic field can induce mixing and pumping (Wilderbeek et al., 2007; Khaderi et al., 2009; Khaderi et al., 2010). Cilia-like structures of micrometer scale have been built by different groups (Singh et al., 2005; Nonaka et al., 2005; Van Oosten et al., 2009; Oh et al., 2009). Anyhow, it was just lately that artificial cilia have could be successfully externally actuated to manipulating fluids on micron scales. Those studies can be divided into two main groups according to the type of produced artificial cilia. The first group of artificial cilia is assembled by a photolithography (Toonder et al., 2008; Fahrni et al., 2009; Schorr et al., 2010; Belardi et al., 2010). Those artificial cilia are of square shape, with a thickness being approximately one order of magnitude less

than width and length such that bending will mainly take place around one axis. Those cilia are oriented parallel to the surface in a totally stretched. The second type of artificial cilia is linear chain of super-paramagnetic particles that are linked with DNA and which have first been used as artificial flagella (Dreyfus, R., 2005). Those structures have similar lengths of up to 30 micro meters while their macroscopic shape is approximately cylindrical. Vilfan et al. (2009) measured the flow induced by the non-reciprocal beating of super paramagnetic particle chains performing an 3D -paddling like motion. Locally induced time averaged velocities could be measured of approximately three micro meters per second at a cilia tip close plane for 1 Hz actuation. Gauger et al. (2009) performed simulations of the flow induced by such beating particle rods indicating that the phase shift of the cilia beat of neighboring cilia significantly influences the pumping performance. Downton et al. (2009) concluded from their numerical investigations that a 3D stroke is much more effective for pumping fluid than a planar stroke.

Anyhow we show that a significant time averaged flow can be induced in a micro channel with a mainly 2D cilia beat cycle that induces significantly faster flow rates than reported by Vilfan et al. (2009). We will show how rotating inhomogeneous magnetic fields induce a cilia beating that leads to a considerable fluid transport.

## **2. Experimental set-up**

The experimental set-up consists of a cilia sample integrated within a channel device; a magnet system is used to actuate the cilia. The measurement set-up enables the measurement of both the cilia motion and the cilia-induced fluid motion during the cilia actuation.

### **2.1. The measurement set-up**

An upright microscope with long working-distance objectives is used for the measurements to enable optical access to the cilia during the actuation. The cilia are observed from the top. Bright-field recordings of the cilia motion and microscopic Particle Image Velocimetry ( $\mu$ PIV) measurements of the cilia-induced fluid motion are performed. A Pegasus-PIV dual head laser serves as light source. Images are recorded with a 12 bit camera of high pixel resolution (1376x1040 pixel) and 9.9 Hz double frame recording rate. The laser and the camera are synchronized with a trigger and timing unit to the actuation phase.

## 2.2. The cilia sample

The cilia are produced on a silicon wafer by photolithography. Iron oxide ( $\text{Fe}_3\text{O}_4$ ) particles are embedded in the polymer matrix (PnBA) of the approximately  $52 \pm 1 \mu\text{m}$  long artificial cilia. Cilia of two different widths are investigated, sketched in Fig. 2a-b.

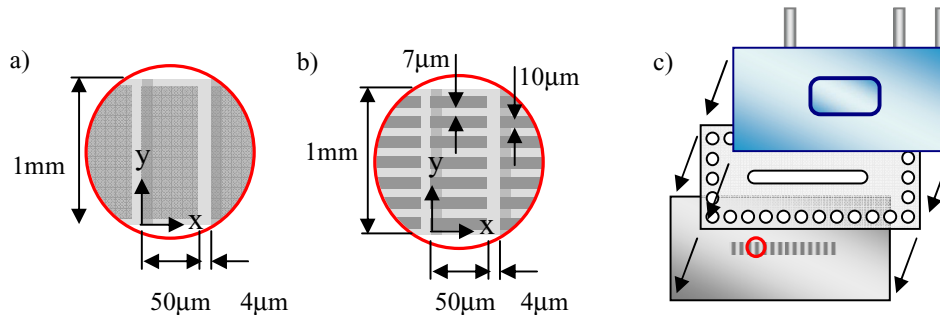


Fig.2 a) Sketch from a top view of cilia that were used for actuation 1 (see section 2.3). The cilia expand over the whole channel width (1 mm). The cilia tips point to the right. b) Sketch of artificial cilia as used for actuation 2 (see section 2.4) from a top view. Approximately 20 cilia of 10 μm width and 7 μm spacing are arranged in spanwise direction. The cilia tips point to the right. c) Sketch of a cilia sample.

The channel is assembled around the sample after the production of the cilia (see Fig. 2c). It consists of three components: (i) the silicon substrate with the cilia, which form the bottom of the channel, (ii) a flexible cartridge which defines the micro channel's width, and (iii) a glass cover with integrated in and outlet connections and a viewing window for good optical access. The cilia are embedded in a sacrificial layer that protects them during the transport and that will be dissolved during the filling of the channel. After the release the cilia are ready for actuation.

## 3. Experimental procedure

In the so-called release process, the micro channel is filled with the working fluid (ethanol or distilled water). The sacrificial layer around the cilia dissolves when getting into contact with the fluid and the cilia are 'released' from their matrix. The filling of the channel takes place such that the cilia root is wetted first and the cilia are horizontally stretched while the sacrificial layer around the microstructures dissolves. After a successful cilia release Rhodamine-B-coated tracers with a 0.91 μm diameter are added to the fluid and micro-PIV measurements are done. The actuation of the magnetic field and the recording sequence are synchronized so that the cilia position is identical at each recorded phase of the actuation cycle.

## 4. Results

### 4.1. Actuation system 1

The actuation system 1 as shown in Fig. 3 consists of a four-coil field generator with amplifiers and a function generator. The micro channel with the cilia substrate is placed in the center between the four pole tips (see Fig. 3.), which create a homogeneous magnetic field that actuated the whole cilia array.

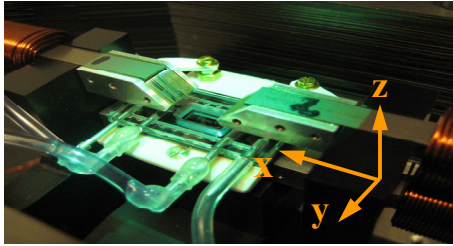


Fig.3: Electromagnet with cilia sample placed between the four pole tips. The actuation system creates rotating and spatially homogenous magnetic fields to actuate the cilia in a synchronic fashion.

The induced field rotates around an axis aligned along the spanwise (y) channel direction. The horizontal and vertical field components shown in Fig. 4a) and 4c) were measured with an amperemeter.

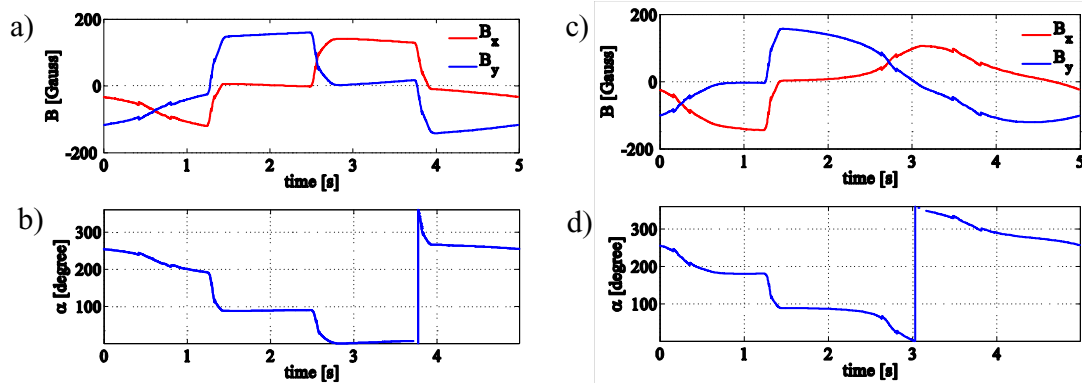


Fig.4: a) Actuation 1a: Magnetic field components during one actuation cycle (T=5 s). b) Actuation 1a: Magnetic field orientation during one actuation cycle. c) Actuation 1b: Magnetic field components during one actuation cycle (T=5s). d) Actuation 1b: Magnetic field orientation during one actuation cycle. 0° equals a horizontal magnetic field orientation along the x-axis.

The horizontal ( $B_x$ ) and vertical ( $B_y$ ) field components as well as the resulting field orientation are shown in Fig. 4. For both actuations the magnetic field rotates counter-clockwise with time-varying angular velocity and strength.

### 4.2. Cilia-induced fluid motion by a uniform, rotating magnetic field

The cilia are actuated at a frequency of 0.2 Hz. Twenty image pairs are recorded during each actuation circle. Velocity fields are computed using PIV by correlation-averaging over a time series of 50 images, which corresponds to 50 actuation cycles. The cilia-induced velocity field in the vicinity of the cilia was measured 50, 100 and 150  $\mu\text{m}$  above the bottom of the channels. Fig. 5a-b shows the median fluid velocities that are calculated for each ensemble averaged vector field.

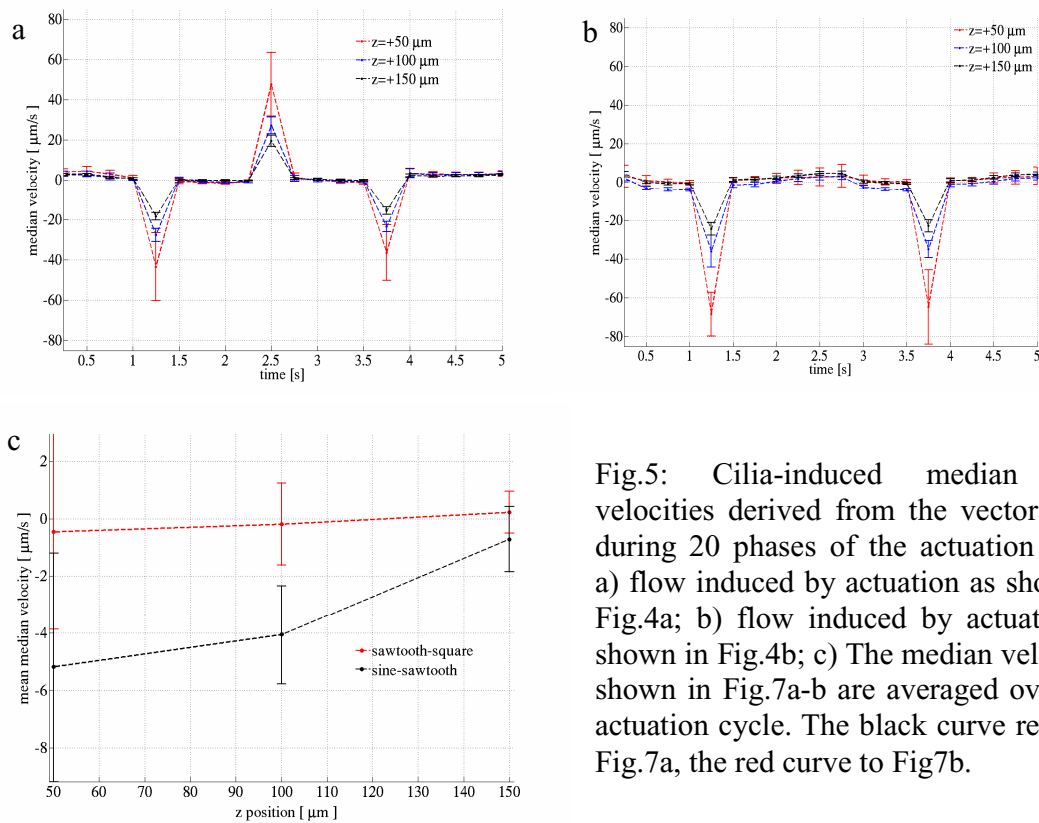


Fig.5: Cilia-induced median fluid velocities derived from the vector fields during 20 phases of the actuation cycle. a) flow induced by actuation as shown in Fig.4a; b) flow induced by actuation as shown in Fig.4b; c) The median velocities shown in Fig.7a-b are averaged over one actuation cycle. The black curve refers to Fig.7a, the red curve to Fig.7b.

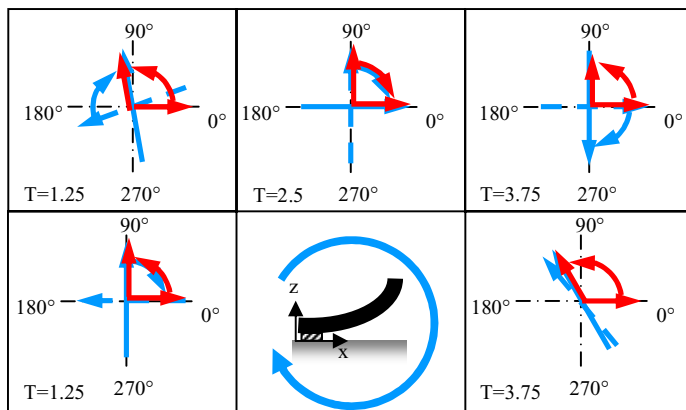


Fig.6: Qualitative sketch from a side view of the cilia orientation indicated in red and the magnetic field orientation indicated in blue during the actuation phases at which cilia perform a rapid motion. Top row for actuation 1a and bottom row for actuation 1b.

During one actuation cycle of 5 seconds 2 or 3 velocity peaks occur. These short phases of fast fluid motion correspond to a collective, rapid motion of the cilia. They can be understood by comparing the field orientation given in Fig. 4 with the induced fluid motion shown in Fig. 5. While the magnetic field rotates  $360^\circ$ , a cilium can align with the field lines only in a restricted way. The bottom allows them a maximum orientation angle which is between  $0^\circ < \alpha < 180^\circ$ . At a certain moment the cilia stops following the field because it is obstructed by the wall. Since the field continues rotating, the cilia will perform a rapid motion against the field rotation sense in order to align with the field again. These phases are reached at  $T=1.25$  s and  $T=3.75$  s which are sketched in Fig. 6 for actuation 1a and 1b. Blue vectors indicate the field orientation, red vectors the cilia orientation. The rapid anticlockwise cilia motion takes place when the magnetic field is oriented between  $120^\circ < \alpha < 180^\circ$ . In Fig. 5a we also recognize a fast fluid motion in

positive x-direction. This is due to a fast collective cilia stroke following the field which rotates at increased speed at this phase ( $T=2.5$  s) as illustrated in Fig. 6a for  $T=2.5$  s. The estimated Reynolds numbers based on the cilia tip velocity and cilia length during the fast stroke is of the order of magnitude of  $Re \sim O(10^{-2})$ . Fig. 5c shows the net velocities averaged over the actuation cycle. It is evident that the net fluid transport rates in all three measurement planes are close to zero. This is due to the fact that the synchronized cilia motion mainly induces a forward-backward motion of the fluid. It is anticipated that a net fluid transport does not take place because the cilia beat cycle lacks the required asymmetry between the forward and the backward stroke.

### 4.3. Actuation system 2

The actuation system 2 consists of a disc that rotates under the sample as shown in Fig. 7. On the disc 5 mm cubic permanent magnets are placed at a middle radial distance of 2.8cm to the rotation axis at an angle interval of  $60^\circ$ .

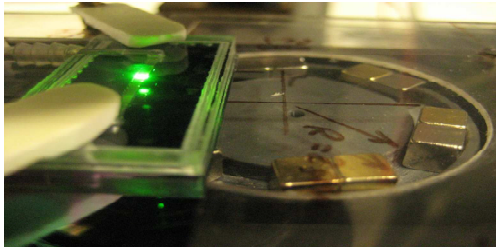


Fig.7: Actuation system 2 consists of permanent magnets that are placed on a rotating disk. The magnetic field actuates the artificial cilia inside the channel, which is placed off axis above the rotating magnets.

The array of cilia experiences a time and space varying magnetic field. The horizontal and vertical field components during an actuation circle are shown in Fig. 8. Note that the magnetic field given in Fig. 8 was measured on the centerline of the magnets. The

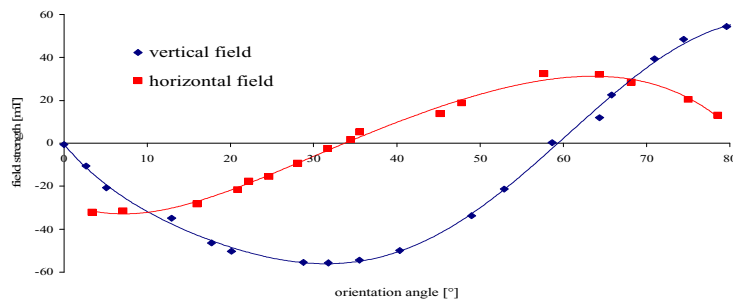


Fig.8: Magnetic field components during the rotation of the disc. Due to the alternating orientation of the magnets, the field has a periodicity of  $120^\circ$ .

field felt by cilia upstream or downstream will be slightly different due to the small radius of the rotating disk. At certain actuation phases, the field direction and strength induced by the permanent magnet is not constant over the array of cilia. This is different from the field induced by the electromagnet, which is homogeneous in direction and strength at any phase of the actuation cycle. The cilia response to the external actuation is illustrated in Fig. 9. The cilia are shown from a top view and are visualized by fluorescent tracers sticking to the edges of the cilia. Figure 9a-9e shows that the cilia perform simultaneously a downward motion, while the upward stroke shown in Fig. 9f-9h is less coordinated, leading to a temporal phase lack of the cilia motion.

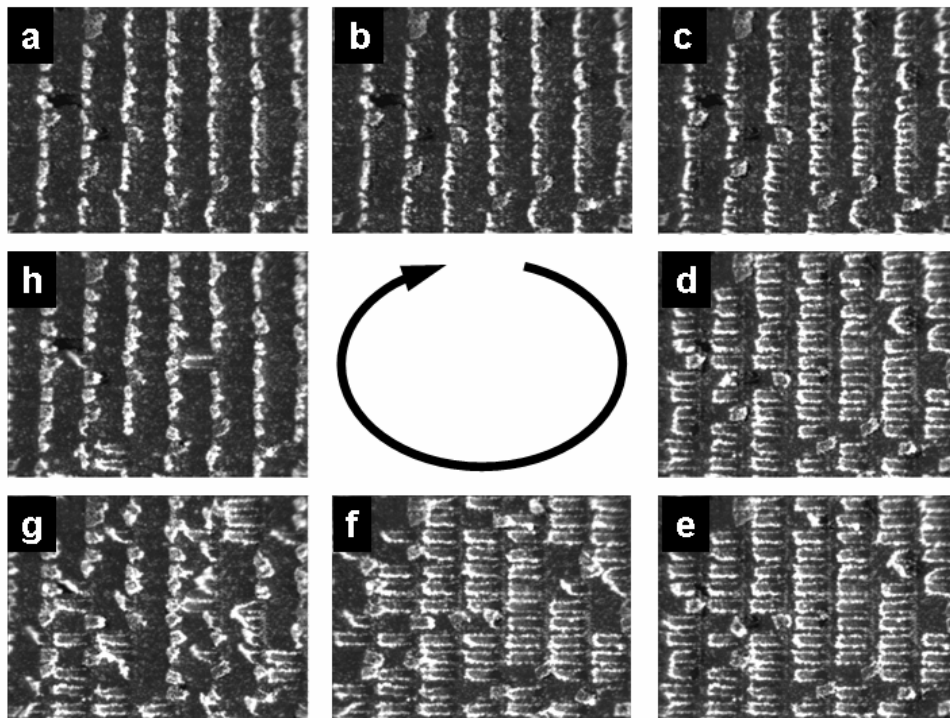


Fig. 9: a-g: different phases of the cilia actuation: a-e) active stroke to the left, f)-h) recovery stroke. The cilia length is approximately 50  $\mu\text{m}$ .

#### 4.4. Cilia-induced fluid motion by a non-uniform, rotating magnetic field

For this experiment the cilia geometry as shown in Fig. 2b was used in the set-up. Phase-locked measurements have been performed such that the actuation frequency was always a multiple of the recording rate. 400 images were acquired in each plane and measurements were performed in 12 equidistantly spaced measurement planes 30 $\mu\text{m}$  apart. The resulting magnetic field at the middle of the micro channel is given in Fig.8. The rotation direction of the field with respect to the cilia orientation is identical as in the first experiment (see Fig.10b), such that cilia will follow the field until they are stretched and perform a rapid counter-clockwise motion against the sense of rotation of the field (Fig. 9). The cilia are now individual elongated structures, such that they can twist out of the xz plane. Furthermore, the magnetic field is inhomogeneous along the micro channel during certain periods of the actuation. The cilia therefore do not move synchronously throughout the actuation cycle. Fig.10a shows the cilia-induced flow over a channel height of  $0 \pm 15 \mu\text{m} \leq z \leq 290 \pm 15 \mu\text{m}$ . The cilia orientation and magnetic field rotation sense are indicated in sketch Fig. 10b. Fig. 10a shows that the spanwise velocities (in y-direction) and the variations of the velocity magnitudes decrease with increasing spacing to the cilia. The flow reverses approximately 3 cilia lengths above the channel bottom ( $z \approx 150\mu\text{m}$ ) as can be seen from Fig. 10c which shows the resulting velocity profile over the channel height. The backflow occurs since the inlets and outlets of the channel are closed during the experiment which results in a reverse flow. The measured velocity profile shows that the artificial cilia induce a fluid transport in the lower half of the micro channel.

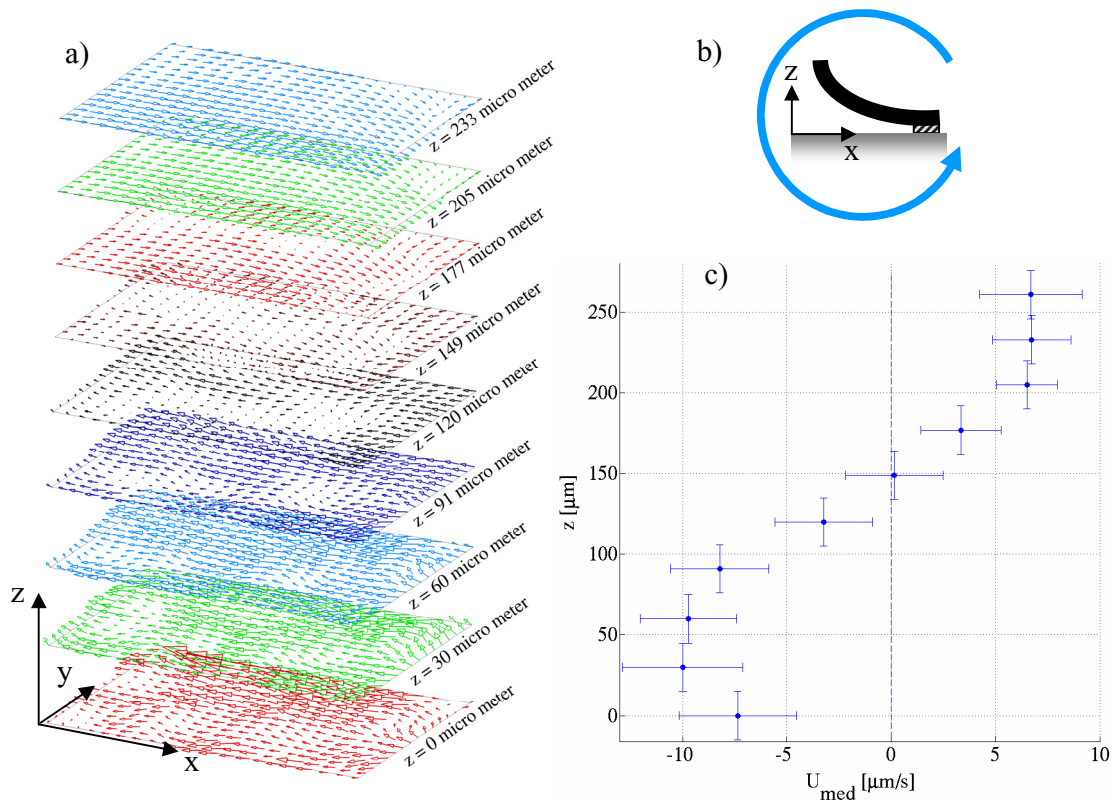


Fig.10: a) Vector fields of the cilia-induced flow for increasing distance to the cilia root position. b) Sketch of the cilia orientation with respect to the rotation sense of the magnetic field; c) median velocities of all measurement planes: Horizontal error bars indicate the median absolute deviation, while vertical error bars indicate the correlation depth of the measurement plane.

## 5. Discussion

A significant artificial-cilia induced fluid transport was achieved by a large numbers of actuated cilia that are integrated into a micro channel. The cilia move in a coordinated fashion and the generated beat cycles is steady over a long time-period.

In this work artificial cilia have been actuated in two different ways. A rotating, spatially homogenous magnetic field was applied to explore cilia-induced fluid transport by a shape asymmetry of the cilia beat. In a second experiment a rotating, spatially inhomogeneous magnetic field was applied to explore cilia-induced fluid transport by metachronal coordination of the cilia beat.

When all cilia move synchronized in a homogeneous field, the flow is dominated by fluid fluctuations. The measured fluid velocities reverse with the forward and backward motion of the cilia and seem to be proportional to the velocity of the cilia beat. The fluid displacement averaged over one cycle is insignificant, indicating that the motion of the shape of the cilia during the forward and backward stroke must be identical. This is confirmed by bright field measurements where no asymmetry in the cilia beat could be observed.

When the cilia are actuated with a rotating, inhomogeneous magnetic field, a continuous

net fluid transport was observed. We anticipate that a net transport effect is induced by the phase lag of the beating of neighboring cilia which is only present during the upward stroke. Since such a local phase shift is absent during the downward motion an asymmetry in the global beating is induced even though individual cilia perform a symmetric beat. The experimental findings are supported by numerical investigations that show that a special phase shift between beating cilia leads to a net fluid transport in the viscous regime even when the individual cilia beat is reciprocal (Hussong et al., submitted 2010).

## **6. Outlook**

Time resolved measurements will give insight in the cilia and fluid motion during a beat cycle. Fluid fluctuations during the actuation cycle can be quantified and compared with the net fluid motion and total as well as the effective drag induced by the beating cilia can be estimated. A detailed study on the cilia motion will allow quantifying the phase lag between the cilia beats and the out-of-plane motion and its dependence on different actuation frequencies.

## **7. Conclusions**

Artificial cilia induced fluid transport was shown in a micro channel. We anticipate that the transport is induced by a combination of phase lagged beating and a weak 3D paddling motion of the cilia.

In contrast, when the cilia beat in a synchronous way an oscillatory fluid motion in the micro-channel is induced which leads to no significant fluid transport. We believe that this is due to the absence of a beat asymmetry in the beat cycle.

## **Acknowledgment**

This work is a part of the European project ARTIC, under Contract No. STRP 033274.

## **References**

- Baltussen, M.G.H.M., Anderson, P.D., den Toonder, J. M. J., 2009. Inertial flow effects in a micro-mixer based in artificial cilia. *Lab on a Chip*, 9, 2326.
- Barton, C. and Raynor, S., 1967. Analytical Investigation Of Cilia Induced Mucous Flow. *Bulletin Of Mathematical Biophysics*, 29, 419, 3.
- Belardi, J., Schorr, N., Prucker, O., Ruhe, J., Wells, S., Patel, V., 2010. 2nd European Conference on Microfluidics – Toulouse, December 8-10, 2010.
- Blake, 1971. Spherical Envelope Approach To Ciliary Propulsion. *JFM*, 46, 199.
- Blake, J. R. and Winet, H., 1980. On The Mechanics Of Muco-Ciliary Transport. *Biorheology*, 17, 125-134, 1-2.
- Blake, J. R., 1971a. Infinite Models For Ciliary Propulsion. *JFM*, 49, 209.
- Blake, J. R., 1972. Model For Micro-Structure In Ciliated Organisms. *JFM*, 1972, 55, 1.
- Brennen, C., 1974. Oscillating-Boundary-Layer Theory For Ciliary Propulsion. *JFM*, 65, 799-824.
- Dauplain, A. and Favier, J. and Bottaro, A., 2008. Hydrodynamics of ciliary propulsion. *Journal Of Fluids And Structures*, 24, 1156—1165, 8.
- den Toonder, J. and Bos, F. and Broer, D. and Filippini, L. and Gillies, M. and de Goede, J. and Mol, T. and Reijme, M. and Talen, W. and Wilderbeek, H. and Khatavkar, V. and Anderson, P., 2008. Artificial

- cilia for active micro-fluidic mixing. *Lab On A Chip*, 8, 533-541, 4.
- Dillon, R. H., Fauci, L. J. and Yang, X. Z., 2006. Sperm motility and multiciliary beating: An integrative mechanical model. *Computers & Mathematics with Applications*, 52, 749—758, 5.
- Dillon, R. H., Fauci, L. J., Omoto, C. and Yang, X. Z., 2007. Fluid dynamic models of flagellar and ciliary beating. *Reproductive Biomechanics*, 1101, 494-505.
- Downton, M.T. and Stark, H., 2009. Beating kinematics of magnetically actuated cilia. *EPL*, 85, 44002.
- Dreyfus, R., Baudry, J., Roper, M.L., Fermigier, M., Stone, H.A. and Bibette, J., 2005. Microscopic artificial swimmers. *Nature*, vol.437,862-865.
- Fahrni, F., Prins, M., van IJzendoorn, L., 2009. Micro-fluidic actuation using magnetic artificial cilia. *Lab Chip* 9, 3413-3421.
- Gauger, E.M., Downton, M.T. and Stark, H., 2009. Fluid transport at low Reynolds number with magnetically actuated artificial cilia. *Eur. Phys. J. E* 28, 231-242.
- Gueron, S. and Levit-Gurevich, K., 1998. Computation of the internal forces in cilia: Application to ciliary motion, the effects of viscosity, and cilia interactions. *Biophysical Journal*, 74, 1658-1676, 4.
- Gueron, S., Levit-Gurevich, K., Liron, N. and Blum, J. J., 1997. Cilia internal mechanism and metachronal coordination as the result of hydrodynamical coupling. *Proceedings Of The National Academy Of Sciences Of The United States*, 94, 6001-6006, 12.
- Heys, J. J., Gedeon, T., Knott, B. C. and Kim, Y., 2008. Modeling arthropod filiform hair motion using the penalty immersed boundary method. *Journal Of Biomechanics*, 41, 977—984, 5.
- Hussong, J., Breugem, W.-P., Westerweel, J. 2010. A continuum model for flow induced by metachronal coordination between beating cilia. *JFM* (submitted).
- Katz, D. F., 1974. Propulsion Of Microorganisms Near Solid Boundaries. *JFM*, 64, 33-49.
- Keller, S. R. and Wu, T. Y., 1977. Porous Prolate-Spheroidal Model For Ciliated Microorganisms. *JFM*, 80, 259.
- Khaderi, S.N., Baltussen, M.G.H.M., Anderson, P.D., Ioan, D., den Toonder, J. M. J., Onck, P.R., 2009. Nature-inspired microfluidic propulsion using magnetic actuation. *Physical Review E*, 79, 046304.
- Khaderi, S.N., Baltussen, M.G.H.M., Anderson, P.D., Ioan, D., den Toonder, J. M. J., Onck, P.R., 2009. 2nd European Conference on Microfluidics – Toulouse, December 8-10, 2010.
- King, M., Agarwal, M. and Shukla, J. B., 1993. A Planar Model For Mucociliary Transport - Effect Of Mucus Viscoelasticity. *Biorheology*, 30, 49—61, 1.
- Klein, M. K., Haberberger, R. V., Hartmann, P., Faulhammer, P., Lips, K. S., Krain, B., Wess, J., Kummer, W., Koenig, P., 2009. Muscarinic receptor subtypes in cilia-driven transport and airway epithelial development. *Eur. Respir. J.*, 33, 1113-1121.
- Knowles, M. R., Boucher, R. C., 2002. Mucus clearance as a primary innate defence mechanism for mammalian airways. *J. Clin. Invest.*, 109, 571-577
- Koenig, P., Krain, B., Krasteva, G., Kummer, W., 2009. Serotonin increases cilia-driven particle transport via an acetylcholine-independent pathway in the mouse trachea. *Plosone*, 4, 3, e4938
- Lenz, P. and Ryskin, A., 2006. Collective effects in cilia arrays. *Physical Biology*, 3, 285—294, 4.
- Liron, N. and Mochon, S., 1976. Discrete-Cilia Approach To Propulsion Of Ciliated Microorganisms. *JFM*, 75, 593-607.
- Liron, N., 1978. Fluid Transport By Cilia Between Parallel Plates. *JFM*, 86, 705-726.
- Matsui, H., Randell, S. H., Peretti, S. W., Davis, C. W. and Boucher, C., 1998. Coordinated clearance of periciliary liquid and mucus from airway surfaces. *J. Clin. Invest.*, 102, 6, 1125-1131
- Niedermayer, T. and Eckhardt, B. and Lenz, P., 2008. Synchronization, phase locking, and metachronal wave formation in ciliary chains. *Chaos*, 18, 037128, 3.
- Nielsen, N. F. and Larsen, P. S., 1993. A Note On Ciliated Plane Channel Flow With A Pressure-Gradient. *JFM*, 257, 97-110.
- Nonaka, S. and Yoshida, S. and Watanabe, D. and Ikeuchi, S. and Goto, T. and Marshall, W. F. and Hamada, H., 2005. De novo formation of left-right asymmetry by posterior tilt of nodal cilia. *Plos Biology*, 3, e268, 8.
- Oh, K., Chung, J.-H., Devasia, S. and Riley, J. J., 2009. Bio-mimetic silicone cilia for microfluidic manipulation. *Lab on a Chip*.
- Purcell, E. M., 1977. Life At Low Reynolds-Number. *American Journal Of Physics*, 45, 3-11, 1.
- Schorr, N., Belardi, J., Prucker, O., Ruhe, J., Wells, S., Patel, V., 2010. 2nd European Conference on Microfluidics – Toulouse, December 8-10, 2010.
- Singh, H., Laibinis, P. E. and Hatton, T. A., 2005. Synthesis of flexible magnetic nanowires of permanently linked core-shell magnetic beads tethered to a glass surface patterned by microcontact printing. *Nano Letters*, 5, 2149—215411.
- Smith, D. J., Gaffney, E. A. and Blake, J. R., 2007. A viscoelastic traction layer model of muco-ciliary

- transport. *Bulletin Of Mathematical Biology*, 69, 289-327, 1.
- Smith, D. J., Gaffney, E. A. and Blake, J. R., 2008. Modelling mucociliary clearance. *Respiratory Physiology & Neurobiology*, 163, 178-188, 1-3.
- Taylor, G., 1951. Analysis Of The Swimming Of Microscopic Organisms. *Proceedings Of The Royal Society Of London Series A-Mathematical And Physical Sciences*, 209, 447-461, 1099.
- Teich, M., 1970. Purkyně and Valentin on Ciliary Motion: An Early Investigation in
- Toonder, J., Bos, F., Broer, D., Filippini, L., Gillies, M., de Goede, J., Mol, T., Reijme, M., Talen, W., Wilderbeek, H., Khatavkar, V., Anderson, P., 2007. Artificial cilia for active micro-fluidic mixing. *Lab Chip* 8, 533-541.
- Tuck, E. O., 1968. A Note On A Swimming Problem. *JFM*, 31, 305.
- Van Oosten, C.L., Bastiaansen, C.W.M., Broer, D.J., 2009. Printed artificial cilia from liquid-crystal network actuators modularly driven by light. *Nature Materials*, vol.8, 677-682.
- Vilfan, A. and Julicher, F., 2006. Hydrodynamic flow patterns and synchronization of beating cilia. *Physical Review Letters*, 96, 058102, 5.
- Vilfan, M., Potocnik, A., Kavcic, B., Osterman, N., Poberjaj, I., Vilfan, A. and Babic, D., 2009. Self assembled artificial cilia. *PNAS* vol.5, no.5, 1844-1847.
- Wilson, G. B., Jahn, T., Fonseca, J., 1975. Studies on ciliary beating of frag pharyngeal epithelium in vitro I. Isolation and ciliary beat of single cells. *T. Am. Microsc. Soc.*, 94, 43-57.